International Journal of Modern Physics B, Vol. 15, Nos. 6 & 7 (2001) 878–885

SHEAR BANDED STRUCTURES AND NEMATIC TO ISOTROPIC TRANSITION IN MR FLUIDS

O.VOLKOVA, G BOSSIS, P.CARLETTO, A.CEBERS*
LPMC,UMR 6622,University of Nice,parc Valrose,06108 Nice Cedex 2

*Institute of Physics,Latvian Academy of Sciences,Salaspils-1,LV-2169,Latvia

ABSTRACT

The experiemental shear stress versus shear rate curves of MR fluids are analysed with the help iof a chain model. Two critical shear rates are found, one corresponding to the onset of agregate breaking and the other corresponding to the total disappearance of aggregates. Above this second critical shear rate we observe an abrupt jump of stress and the onset of a layered stripe pattern This novel shear induced transition can be observed by using a cone-plate geometry but is usually smeared out in a plate-plate geometry . Still in a plate plate geometry we also have observed a similar phase separation in ER fluids but without a clear rheological signature. We show that this phase separation can be explained by the transition from a nematic like order induced by the field to an isotropic state which is obtained when the shearing hydrodynamic forces on a pair of particles overcome the magnetic or electrostatic forces. The critical shear stress predicted on this basis is in good agreement with the experimental results. We find a similar layered pattern in a rotating magnetic field. The connection between the two situations is explained .

1.Introduction

Besides the interest for applications of magnetorheological suspensions (MRS) which can show yield stresses as high as 100kPa[1], they are interesting fluids in order to study flow and field induced phase separation. A magnetic fluid at rest, will undergo a phase separation when the dipolar energy will become larger than the thermal energy. Due to a competition between long range repulsive and short range attractive magnetic interactions, the phase separation will give rise to some pattern for the dense phase: the long range repulsive forces tends to split the matter in order to reduce the repulsive energy whereas attractive forces such as those giving rise to surface tension or Lorentz field tend to gather the matter in a single unit. In magnetic liquids it is possible to successfully predict the change of period of a striped pattern with the amplitude of the external magnetic field, if the effective surface tension at the boundary between the two phases is known[2]. More recently, pattern formation has been observed in electro and magnetorheological suspensions which are suspensions of much larger (1-10 μm) paramagnetic or dielectric particles. Well defined structures formed of cylindrical aggregates aligned on the magnetic field and arranged on an hexagonal pattern have been observed in M.R. fluids at low volume fraction[3,4].The transformation of these cylindrical structures into a striped pattern in the presence of an alternating shear flow has been observed both in M.R. and E.R. fluids[5,6].In this paper we want to focus on the rheology of MRS in shear flows obtained with a cone-plate geometry. The advantage of this geometry on the more usual plate-plate geometry is to ensure a constant shear rate inside the gap which has allowed to find a new shear induced phase separation[7]. In this paper we analyse the rheological curves obtained for different MRS suspensions with the help of the chain model. We shall also present some experimental results about striped structures obtained

with MRS placed in a rotating magnetic field. and will show the connection with the case of steady shear flow.

2.Chain model

In the presence of shear forces, the aggregates of particles, which initially fill the cell, will be progressively destroyed. Then, the important quantity to know is the characteristic size and shape of the aggregates as a function of the shear rate. The control parameter is the shear rate, or in dimensionless form the Mason number, M_n, which is the ratio of the hydrodynamic force due to the shear ($F_{sh} = 6\pi\eta_0\dot{\gamma}a^2$) to the magnetic force between two dipoles at contact (r=2a) with their line of center perpendicular to the direction of the field : $F_m = 0{,}75\pi\mu_0\mu_F a^2\beta^2H^2$. The Mason number is then given by :

$$M_n = \frac{8\eta_0\dot{\gamma}}{\mu_0\mu_F\beta^2H^2} \qquad (1)$$

To our knowledge, all the microstructural models are based on structural units which are either chains of spheres[8] or ellipsoidal aggregates[9]. The calculation method amounts in finding the angle of inclination and the length of the aggregates for a given Mason number, and then to calculate the stress for a suspension of these (non interacting) aggregates.

Considering a chain of spheres as a slender body , the equilibrium angle, θ_e , is obtained from a balance between the hydrodynamic torque and the electro or magnetostatic torque. The condition of stability is obtained by stating that the radial hydrodynamic force at the center of the chain must be lower than the radial attractive force between two adjacent particles. The equations obtained are respectively:

$$\mathrm{tg}\theta_e = \frac{1}{9f_\Gamma\beta^2}\cdot\frac{(l/a)^2}{\ln\frac{2l}{a}}\cdot Mn \qquad (2)$$

$$\frac{Mn(l/a)^2}{\ln\left(\frac{2l}{a}\right)} \le 12\beta^2\,\frac{\left(2f_{//}\cdot\cos^2\theta - f_\perp\sin^2\theta\right)}{\sin(2\theta)} \qquad (3)$$

The quantities $f_{//}, f_\Gamma, f_\perp$ are those appearing in the calculation of the field induced forces between two spheres at contact[10]; they are equal to unity in the dipolar approximation. It is important to note that the two relations for the equilibrium of torques (Eq.2) and of tensile forces (Eq.3) have the same dependence in $M_n(l/a)^2$. It implies that, whatever the length of the aggregates and whatever the Mason number, a chain will be stable if:

$$\mathrm{tg}\theta_e \le \frac{4}{3f_\Gamma}\,\frac{\left(2f_{//}\cdot\cos^2\theta_e - f_\perp.\sin^2\theta_e\right)}{\sin(2\theta_e)} \qquad (4)$$

The equality in Eq.(4) defines a critical angle θ_c above which all the chains, (again whatever their length and whatever the Mason number) will break. The critical angle obtained from Eq (4) is then:

$$tg\theta_c = \sqrt{\frac{4f_{//}}{3f_\Gamma}\left(\frac{1}{1+\frac{2f_\perp}{3f_\Gamma}}\right)} \qquad (5)$$

In the dipolar case ($f_{//}=1$ $f_\Gamma=1$ and $f_\perp=1$) Eq. (5) gives $tg\theta_c=\sqrt{4/5}$ (θ_c=*41,8* degrees) but using the multipolar method we find for $\alpha=\mu_p/\mu_f$=10 (with $f_{//}=7.28$ $f_\Gamma=1.5$ and $\mathbf{f}_\perp=0.62$) θ_c=*66* degrees and for α=*0.1* (with $\mathbf{f}_{//}=0.5967$ $\mathbf{f}_\Gamma=0.9478$ and $\mathbf{f}_\perp=1.969$) θ_c=*30,7* degrees. We see indeed that the critical angle can be quite sensitive to the permeability of the particles.

In this model, the aggregates with an initial length equal to the thickness of the cell begin to rotate in the shear flow(they do not extend to keep an affine motion) and reach the critical angle θ_c. At this angle which corresponds to a first critical Mason number obtained from Eqs (2) and (5):

$$M_n^{c0}=9f_\Gamma\beta^2\frac{\ln(h/a)}{(h/2a)^2}\sqrt{\frac{4f_{//}}{3f_\Gamma}\frac{1}{1+\frac{2f_\perp}{3f_\Gamma}}} \qquad (6),$$

they break in two equal parts and rotate backwards because the hydrodynamic torque has been divided by eight whereas the magnetic one has only been divided by two. Then, increasing the shear rate, we shall reach again the critical angle, the aggregates will break again in two equal parts which will rotate backwards and so on till we reach the state of isolated particles.

The stress on a slender body is given by[11].

$$S_{YZ}=\frac{4\pi\eta_0}{3}\frac{l^3}{\ln(2l/a)}\dot{\gamma}\cos^4\theta \qquad (7)$$

Then, once the initial aggregates have reached the critical angle, the stress is given by Eq.7 with $\theta=\theta_c$ and the viscosity is obtained from the total stress:

$$\eta\dot{\gamma}=\eta_0\dot{\gamma}+\frac{N_a S_{YZ}}{V} \qquad (8.)$$

where $\frac{N_a}{V}$ is the number of ellipsoidal aggregates per unit volume.

Using Eqs.(6)-(8) to relate the shear stress to the shear rate with $l/a=N$ the number of particles in the chain, and Φ the initial volume fraction we get:

$$\frac{\eta}{\eta_0} = 1 + 9\Phi \frac{\beta^2 f_\Gamma \mathrm{tg}\theta_c}{\left(1+\mathrm{tg}^2\theta_c\right)^2} \mathrm{Mn}^{-1} \qquad (9)$$

We see that the chain model predicts a Bingham law in the interval of Mason numbers corresponding to a state where the size of the chains of spheres is reduced from the thickness of the cell to the size of a particle, that is to say for $\mathbf{M_n^{c0}} < \mathrm{Mn} < \mathbf{M_n^c}$. The first critical Mason number corresponds to the first size reduction of the chains and the second to the last division of aggregates. This second critical Mason number can be obtained more exactly than in the slender body theory by writing the balance of tangential and radial forces acting on a pair of spheres :

Taking the origin at the center of gravity of the two spheres we obtain for the force on one particle in the limit of vanishing separations:

$$\vec{F}_H \approx 6\pi\eta\dot{\gamma}a^2\left[2.038\sin\theta\cos\theta\vec{e}_r + 1.6\cos^2\theta\vec{e}_\theta\right] \qquad (10)$$

On the other hand the magnetic (or electrostatic)force on a particle in the presence of a second one has been calculated from a multipolar development :

$$\vec{F}_m = 0.75\pi\mu_0\mu_F\beta^2 a^2 H^2\left[(2f_{//}\cos^2\theta - f_\perp \sin^2\theta)\vec{e}_r + f_\Gamma \sin 2\theta\vec{e}_\theta\right] \qquad (11)$$

In Eqs. (10),(11) $\vec{\mathbf{e}}_\mathbf{r}$ and $\vec{\mathbf{e}}_\boldsymbol{\theta}$ are respectively the unit vectors parallel and perpendicular to the vector joining the centre of the two spheres. As for slender bodies, equating the tangential and radial parts of (10) and (11) allow to get simple expressions for the equilibrium angle and the stability criteria. The critical Mason number is then:

$$M_n^c = \frac{8\eta\dot{\gamma}_c}{\mu_0\mu_F\beta^2 H^2} = \frac{1.581\sqrt{f_{//}f_\Gamma}}{\sqrt{2.038 + 0.8\frac{f_\perp}{f_\Gamma}}}. \qquad (12)$$

Although this expression is more appropriated than the one obtained with the slender body theory, we have neglected the intrinsic torque component since we consider only the torque coming from the total force at the center of each sphere.

To sum up the chain model we see that it predicts a first shear thinning behavior-due to the term $\cos\theta^4$ in Eq.(7) ,then the aggregates reach $\theta = \theta_c$ for $\mathrm{Mn} = \mathrm{M_n^{c0}}$ and the viscosity follows a Bingham behavior (Eq.9) till we reach $\mathrm{Mn} = \mathrm{M_n^c}$ where all the aggregates have disappeared. After this point the chain model no longer applies and we are going to see that the suspension becomes unstable after this point.

3.Experimental results in shear rheometry

We are going to present results obtained with two kinds of suspension. The first one is made of polystyrene particles containing inclusions of magnetite with an average diameter of 0.5 μm and a standard deviation of 10% measured by light scattering. They

are suspended in a mixture of water and glycerol in order to increase the zero field viscosity. The particle initial permeability has been found to be (μ_i=1.7) by using an effective medium theory. The second one is a suspension of carbonyl iron piarticles with an average diameter of 2μm and high initial permeability (μ_i~200).
The experiments were carried out with a rheometer Carrimed CSL100 surrounded by two large Helmotz coils . The field is constant to better than 1% on the size of the cell. Transparent cones allow to see the structures with a video microscope equipment.

3-1 Low shear rate domain

The first graph (fig.1) shows the beginning of a rheogram for a suspension of carbonyl iron at a volume fraction Φ=5% and different fields ranging from 7.6 to 20.7 kA/m. This was recorded in a transparent cone-plate geometry and trans. For every field ,except the lowest one ,there is a change of slope which is due to the transport of thin aggregates and their gathering in larger and denser ones, up to about Mn~0.003. Above these thick

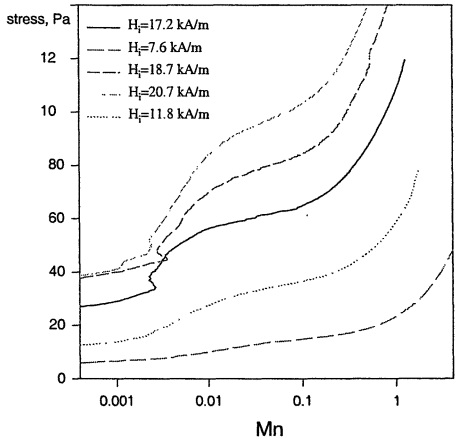

Figure.1 Rheogram for carbonyl iron in coneplate geometry

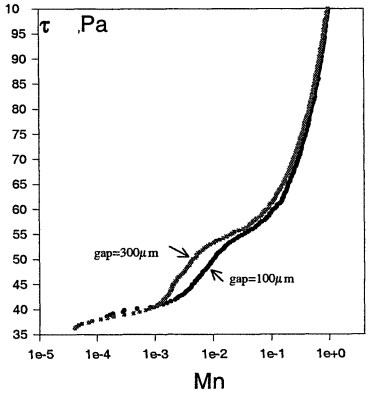

Figure.2 H=18.7 kA/m with two different gaps

aggregates begin to incline and the differential viscosity to decrease. Then at Mn~0,02-0.04 the curvature is inverted and we begin to reach the Bingham regime. We identify this change of curvature with the first rupture of aggregates at the Mason number M_n^{c0}. There is an other reason to believe that this change of curvature correspond to the first rupture of aggregates:, if we use two cells of different heights (but with a plate-plate geometry) we do not obtain the same curve. It is shown in Fig.2 for a field of 18.7 kA/m. The curve shifted towards the left correspond to the largest gap whicht is coherent with Eq.6 since a larger value of h gives a lower critical Mason number. Furthermore we recover the right order of magnitude since in the dipolar approximation $\mathbf{M_n^{c0}}$=0.016 for h=100μm . It is also interesting to note that the curves are smoother than in Fig 1. For the same field. This is because the shear rate is not constant throughout the cell in a plate-plate geometry.If the curves presented in Fig.1 are plotted on a Log-Log scale with $\tau/\eta_0\dot{\gamma}$ on the vertical axis, then all the curves collapse on the same straight line for

$M_n^{c0} < M_n < 1$. The slope of this line is not exactly −1 as in a Bingham model but -0.86 ± 0.02

3.2 Isotropic domain

When all the aggregates have been broken by the shear ($Mn > M_n^c$) we enter in an other regime where the suspension should be isotropic on a mesoscopic scale. Taking the dipolar approximation in Eq.12 we find that it should occur for roughly Mn>1.

In Fig 3 we show the rheogram of a suspension based on magnetic polystyrene in a mixture of water and glycerol for a volume fraction Φ=0.047 and a field H=440 Oe. We can see that, above a critical shear rate (γ_c=68s^{-1})we actually observe a transition in the rheogram with a well marked jump in the shear stress and the onset of a mesoscopic striped structure (cf insert). The period of this structure depends on the height of the cell and is larger on the outer rim with a value d=25μm for a height of 300μm. This structure persists at high shear rates (at least up to 1000s^{-1}) and the period does not change appreciably either with the shear or with the magnetic field. When the stress is decreased we observe a quite strong hysteresis with the persistance of the striped structure till we reach the point where the loading and unloading curves join each other. The same kind of behavior is found for other magnetic fields. It is worth noting that this jump of stress at a critical shear rate is not observable in a plate-plate geometry because the shear rate is not constant throughout the cell. Furthermore, even in a cone-plate geometry ,the observation of this transition is quite sensitive to misalignments or change of distances between the truncated part of the cone and the plate

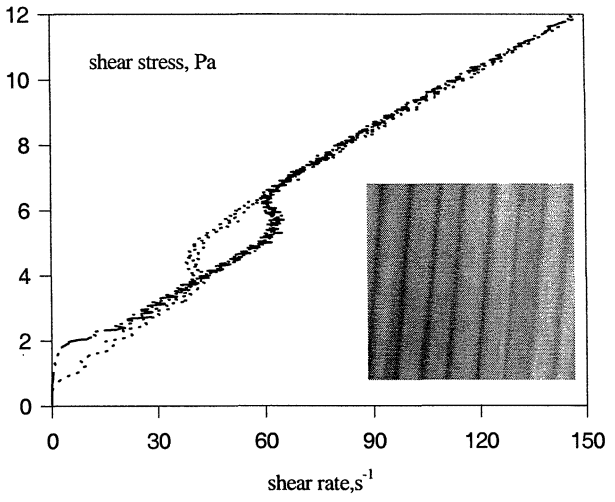

Figure 3. Stress versus shear rate for a magnetic suspension in cone-plate geometry (H=440Oe)

We can verify that this transition is associated with the second critical Mason number by comparing the experimental shear rate associated to the transition to the one

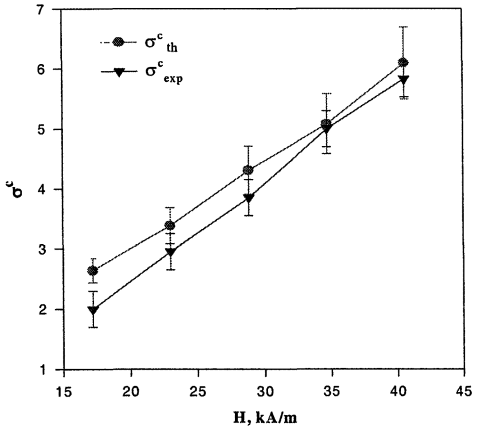

Figure.4 Experimental and theoretical critical stress

predicted by Eq.12. Actually Eq.12 applies in the limit of infinite dilution. More generally we can use an effective medium theory by saying that the stress which is imposed on a given pair of particles, is the total stress acting on the suspension. So we shall replace in Eq.(12). $\eta\dot{\gamma}_c$ by the actual stress σ_c characterizing the transition. Then taking μ_p=1.7 as a representative value for the permeability of the magnetic particles, the values of $f_{//}$, $f_{\perp}$, f_{Γ},are respectively 1.351,0.855,1.059 and Eq.(12) becomes:

$$\sigma_c = \frac{1.15}{8}\mu_0\mu_F\beta^2H^2 \quad (13)$$

The factor 1.15 instead of unity accounts for higher multipoles than the dipolar interaction. In Fig.4 we show the comparison between the prediction of Eq.13 and rhe experiment. We see that the agreement is quite good and confirms that the transition is associated to the total disappearance of the aggregates.

4.Experimental results obtained with a rotating field.

When the shear rate has destroyed the nematic like order we should have an homogeneous suspension ,but actually this situation is unstable since the magnetic energy can be lowered by forming a striped structure which, of course, must remain compatible

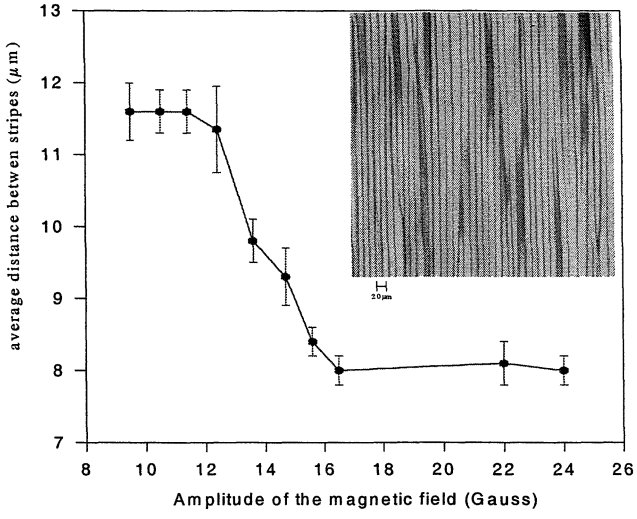

Figure 5: Period of stripes versus the amplitude of the rotating field

with the velocity lines –that is to say in the plane of the velocity and velocity gradient. An equivalent situation happens in the case of a rotating field where the frequency of rotation of the field is high enough for the pair of particles does not move appreciably during a period, then we have an average interaction which is attractive in the plane of the rotating field. Actually the average energy of two dipoles rotating in phase with the magnetic field is $U=-(m^2/2r^3)(1-3\cos^2\theta)$ where θ is the angle between the vector $\vec{r}$ joining the two

dipoles and the normal to the plane of the rotating field. This is just the opposite interaction of two parallel dipoles of strength $m/\sqrt{2}$ whose direction makes an angle θ with $\vec{r}$. This interaction is responsible for the formation of disks of particles in the plane of rotation of the field [12] .Based on this interaction energy it is possible to predict the formation of a layered pattern with the normal to the layers parallel to the axis of rotation of the magnetic field (which plays the role of the vorticity in the shear flow)[13]. We have realized the experiment with the suspension based on magnetic polystyrene particles at a volume fraction of 0.047%. The result is shown in Fig. 5 for the period of the layered pattern versus the amplitude of the rotating magnetic field. In the insert we have a picture of the layered pattern. with a period which will be determined by the demagnetizing field and the size of the particles. The period decreases significantly for a field H~ 13 Oe and then remains constant and equal to 8μm for a cell height h=75μm. The decrease of the period for H~13 Oe corresponds to the onset of phase separation in a constant magnetic field. The period of 8μm is three times smaller than the one obtained in the presence of a shear flow but ,in the cone cell, the height varies between 50μm and 300μm and the period in a constant field is known to increase with the square root of the height. Despite this correction, this period still appears lower than in the case of the shear flow but a more systematic comparison with the use of a plate-plate geometry should help us to conclude on this point.

5.Conclusion

We have shown that the chain model allows to define three regimes in the rheogram which are delimited by two critical Mason numbers (Eqs 6 and 12) and that above the second Mason number the suspension is always unstable with the formation of a layered structure. This layered structure is similar to the one we can observe in a rotating field where the plane of rotation replaces the plane of shear. A detailed comparison of the periods in both cases is being carried out.

6. References

1. J.M.Ginder, L.C.Davis, L.D.Elie in Electro-Rheological fluids, Magneto-Rheological suspensions and associated technology, edited by W.A.Bullough (World scientific, Singapore),1996,603
2. A.Cebers Magnitnaya Gidrodinamika-.3-(1990)-.49
3. E.Lemaire,G.Bossis,Y.Grasselli J.Phys. II. **2** (1992) 359
4. J.Liu &al. Phys.Rev.Letters **74**(1995-P.2828
5. S.Cutillas,G.Bossis,A.Cebers. Phys.Rev.E.**57** (1998).804
6. S.Cutillas,G.Bossis Europhys.Lett. **40** (1997)465
7. O.Volkova,S.Cutillas,G.Bossis, Phys.Rev.Letters 82 (1999) 233-236
8. J.E.Martin and R.A.Andersen, *J.Chem.Ph.* **104**, (1996) 4814,
9. Shulman Z.P., Kordonsky V.I., Zaltsgendler E.A., Prokhorov I.V., Khusid B.M., Demchuk S.A., *Int. J. Multiphase flow,* **12**, (1986) 935
10. -Klingenberg D.J.;Zukoski C.F., *Langmuir*,**6** (1990).15-24
11. G.K.Batchelor, *J.Fluid; Mech.*, **44**, (1970)419
12. T.C.Halsey, R.A.Anderson, J.E.Martin in ER fluids,MR suspensions and associated technology p192,W.A.Bullough ed.,World Scientific,Singapore 1996
13. A.Cebers,G.Bossis, JMMM (1999) to appear